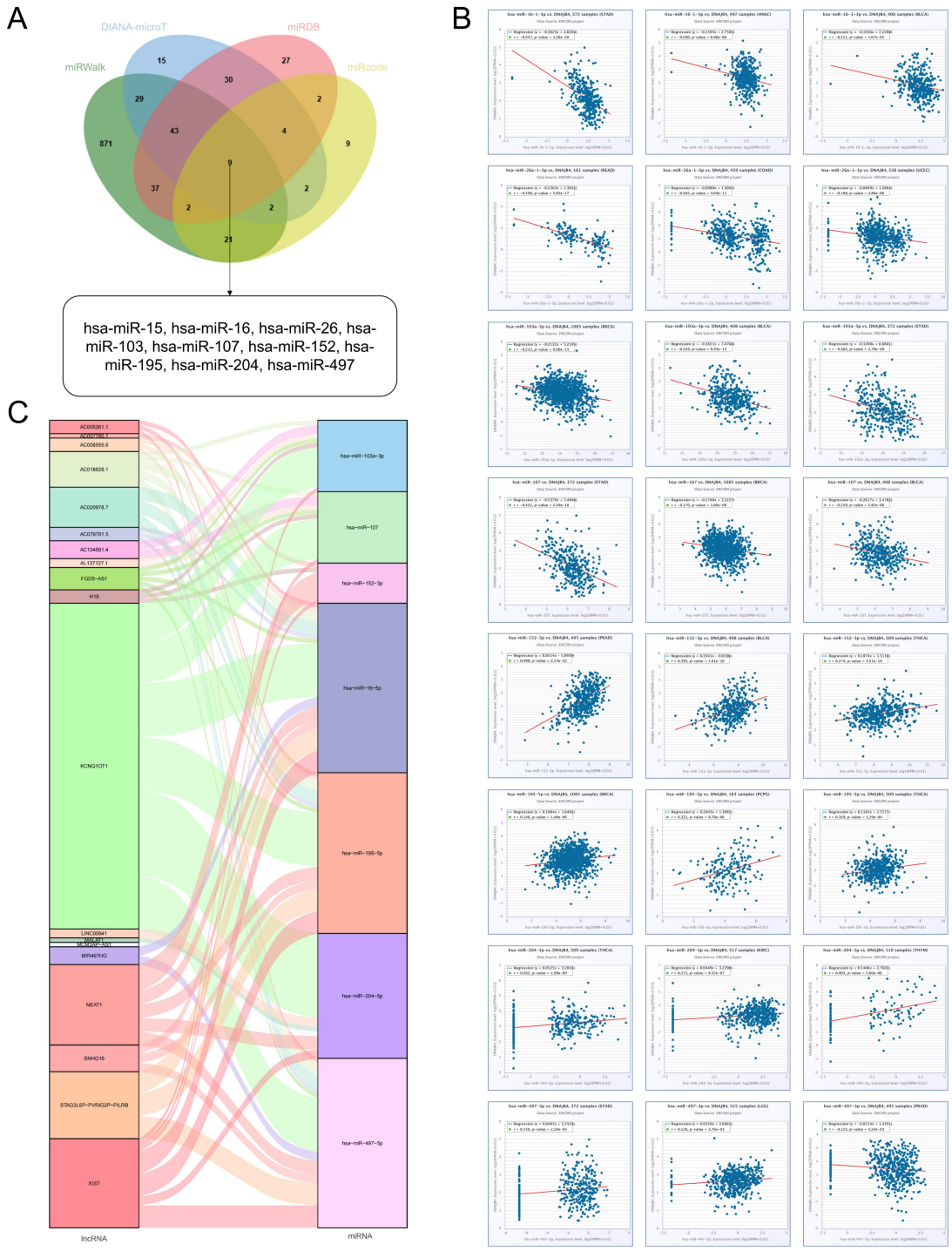

Figure S1. CeRNA Analysis of DNAJB4

(A) By taking the intersections from miRWalk, DIANA-microT, miRDB, miRcode database, we identify hsa-miR-15, hsa-miR-16, hsa-miR-26, hsa-miR-103, hsa-miR-107, hsa-miR-152, hsa-miR-195, hsa-miR-204, and hsa-miR-497 as key miRNAs targeting DNAJB4.

(B) The correlations between the expressions of key miRNAs and DNAJB4 were illustrated in the scatter plots.

(C) The Sankey diagram exhibited the associations of lncRNA and miRNA.

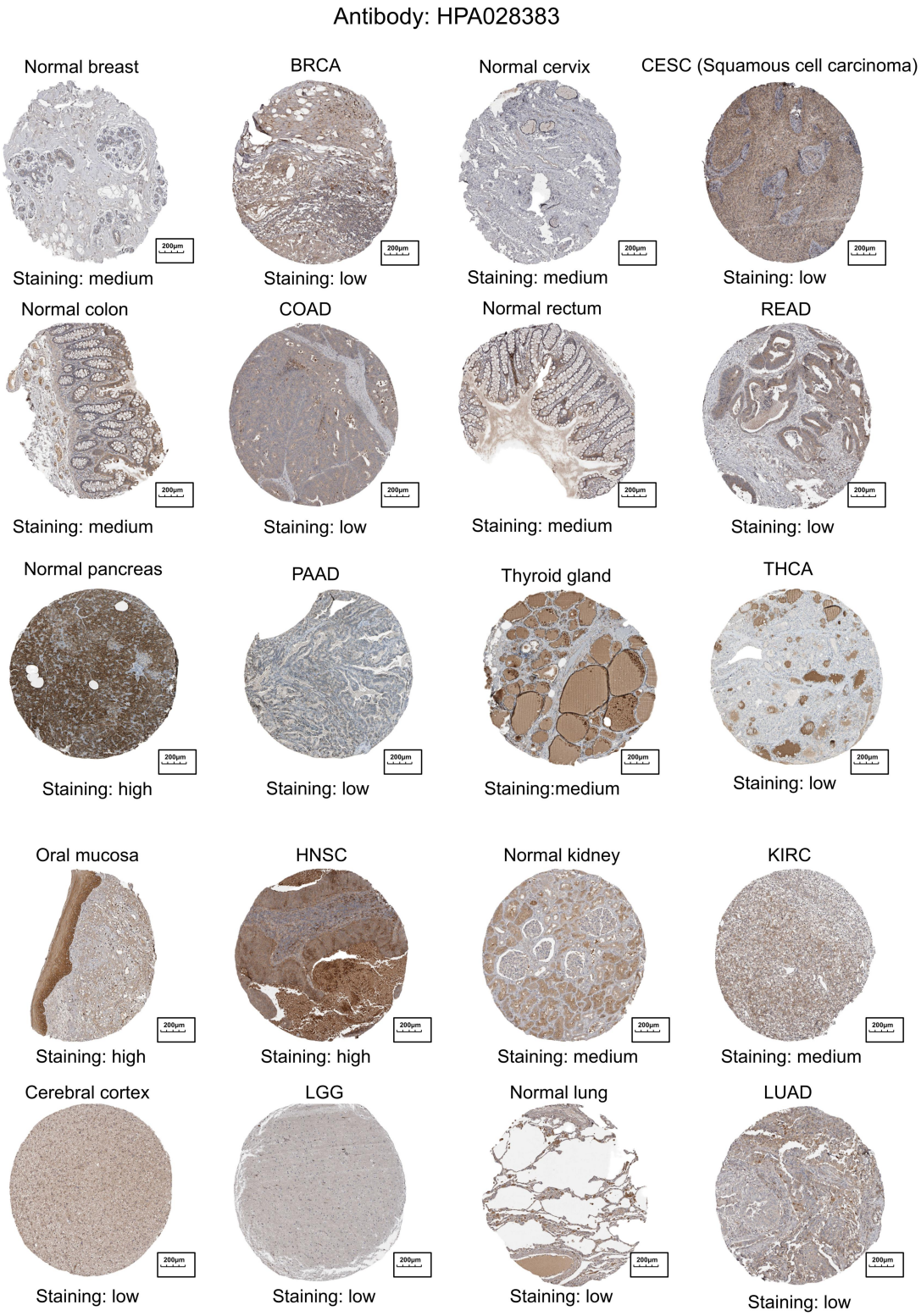

Figure S2. IHC staining of DNAJB4 in various tumor and normal tissues of human.

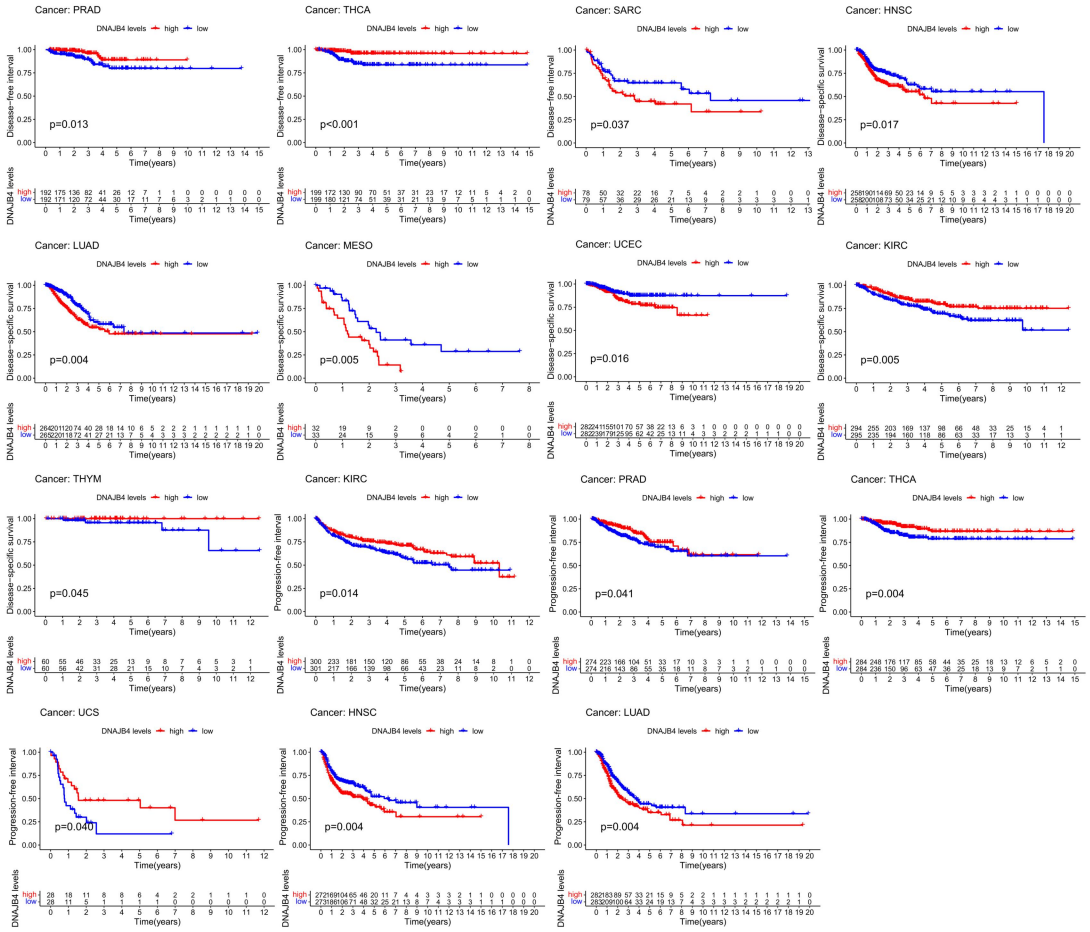

Figure S3. Kaplan-Meier survival analysis of DNAJB4 in pan-cancer.

The expression of DNAJB4 showed a positive correlation with DFI in PRAD (P-value = 0.013) and THCA (P-value < 0.001), while exhibiting a negative correlation in SARC (P-value = 0.037). In terms of DSS, high DNAJB4 expression was significantly associated with low DSS in HNSC (P-value = 0.017), LUAD (P-value = 0.004), MESO (P-value = 0.005), and UCEC (P-value = 0.016). Conversely, it correlated with high DSS in KIRC (P-value = 0.005) and THYM (P-value = 0.045). Additionally, elevated DNAJB4 expression was significantly linked to high PFI in patients with KIRC (P-value = 0.014), PRAD (P-value = 0.041), THCA (P-value = 0.004), and UCS (P-value = 0.040) but corresponded to low PFI in those with HNSC (P-value = 0.004) and LUAD (P-value = 0.004).

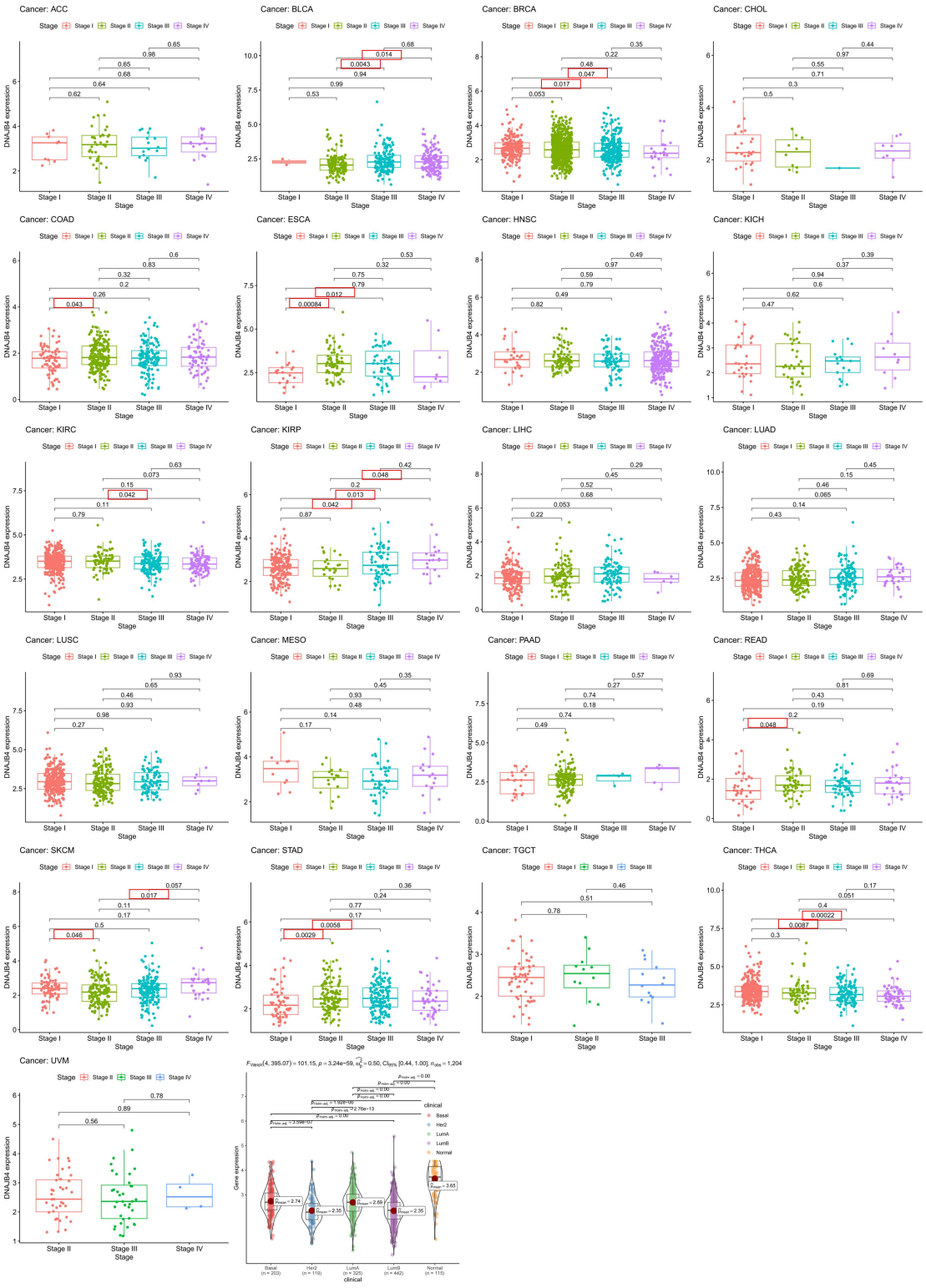

Figure S4. Correlation between DNAJB4 and clinical staging and tumor heterogeneity in pan-cancer.

In BRCA, KIRC, and THCA, the expression levels of DNAJB4 demonstrated a significant negative correlation with clinical staging. In contrast, in KIRP and READ, a positive

correlation between DNAJB4 expression and clinical staging was identified. Additionally, the expression levels of DNAJB4 revealed heterogeneity across distinct molecular subtypes of BRCA.

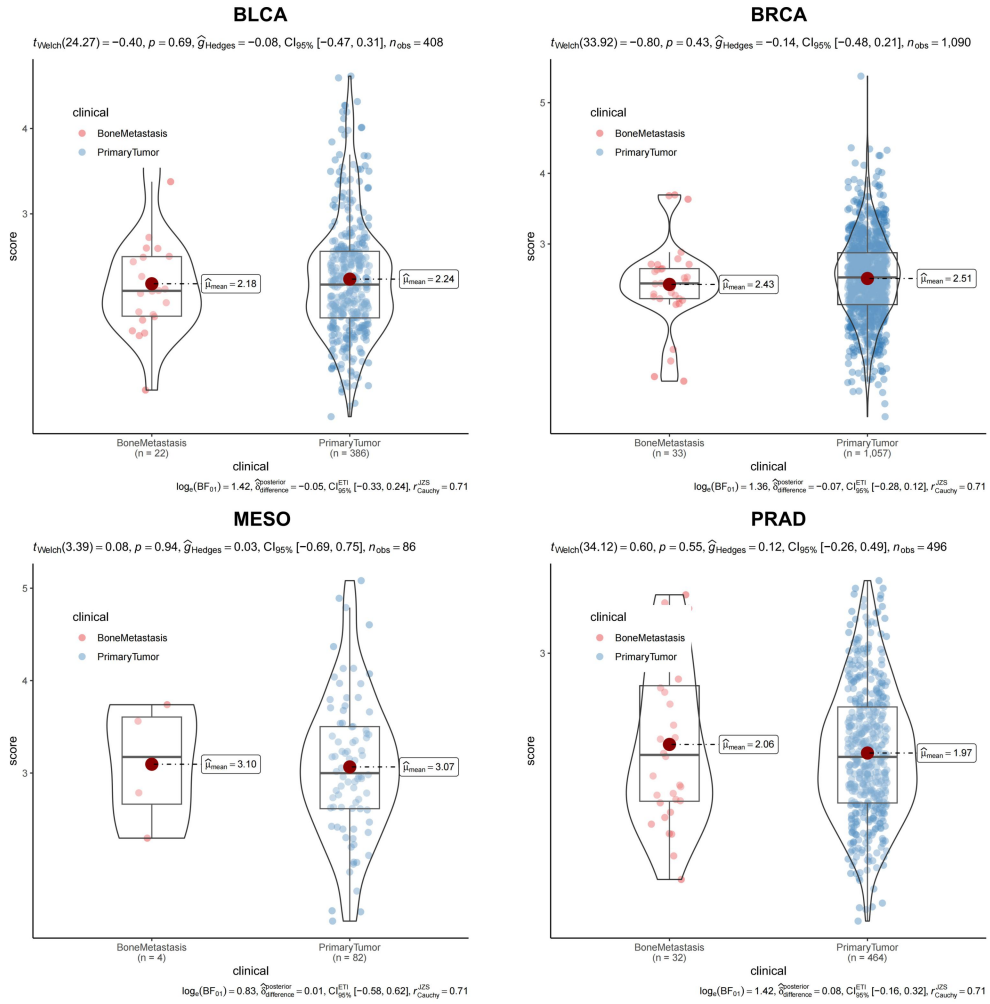

Figure S5. Correlations of DNAJB4 with bone metastasis.

The expression levels of DNAJB4 did not demonstrate significant differences between primary tumors and bone metastases across the four tumor types: BLCA, BRCA, MESO, and PRAD, with corresponding P-values of 0.69, 0.43, 0.94, and 0.55.

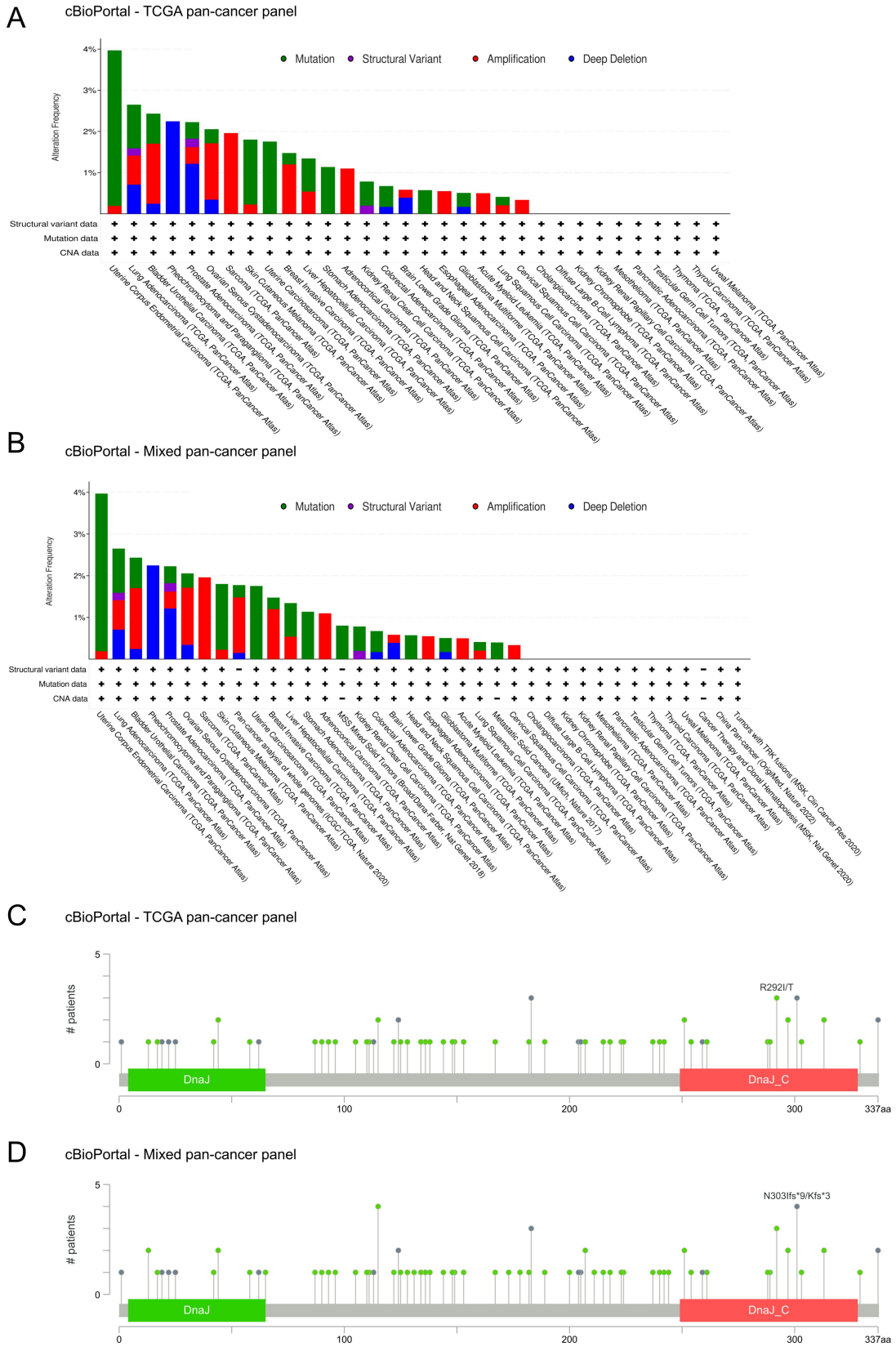

Figure S6. DNAJB4 variants in pan-cancer.

The plot presented a comprehensive analysis of DNAJB4 variations across diverse cancer types (A-B) and identified the specific mutation sites associated with the gene (C-D).

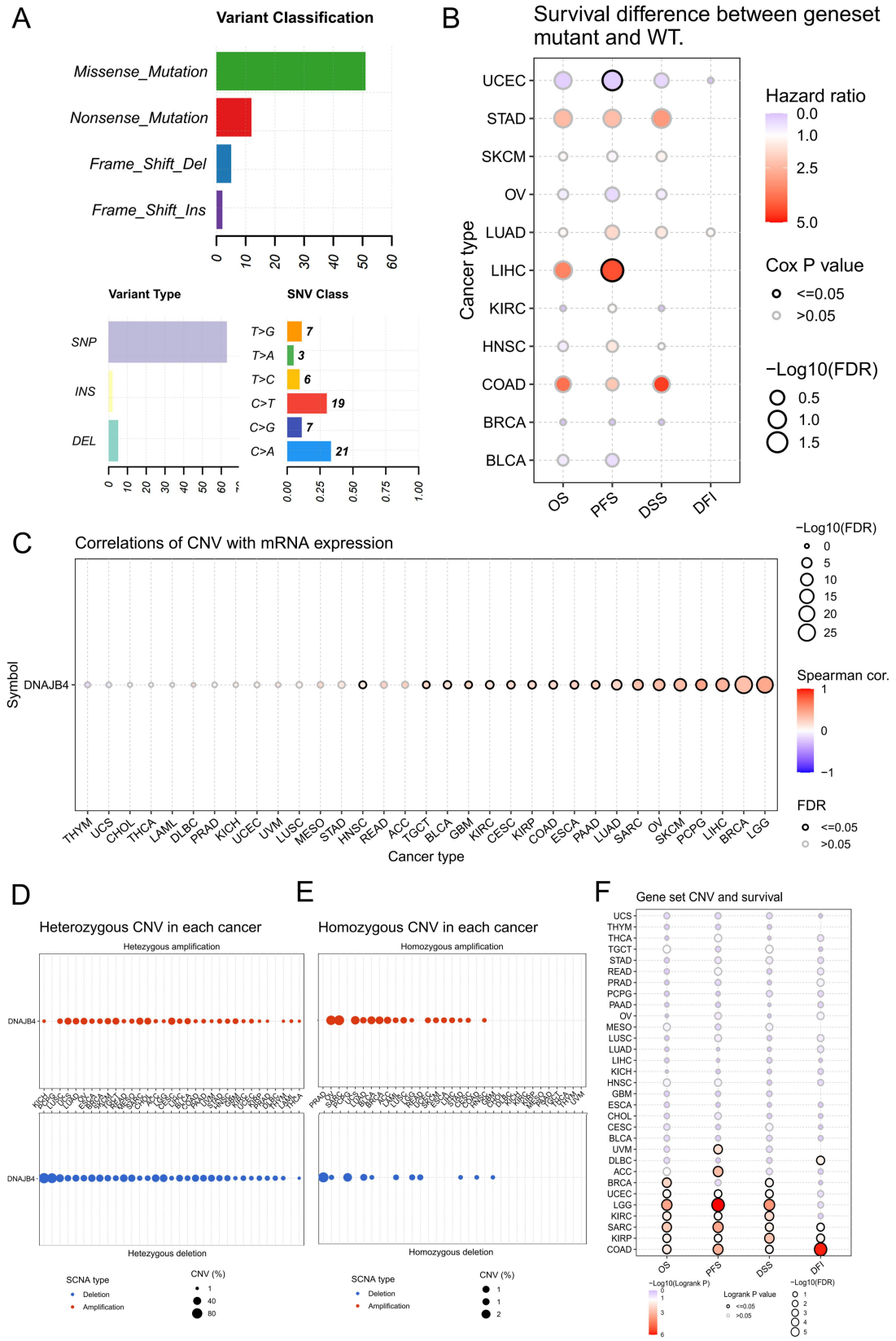

Figure S7. Relationships between DNAJB4 and mutations as well as CNV.

(A) Missense mutations constituted the predominant category of SNVs, with “C>A” being the most frequently encountered variant type.

(B) The DNAJB4 mutation demonstrated a protective role in UCEC, whereas it functioned as a prognostic risk factor for PFS in LIHC.

(C) The CNV of DNAJB4 was significantly positively correlated with mRNA expression levels in HNSC, TGCT, BLCA, GBM, KIRC, CESC, KIRP, COAD, ESCA, PAAD, LUAD, SARC, OV, SKCM, PCPG, LIHC, BRCA and LGG.

(D) The frequency of heterozygous deletion of the DNAJB4 gene was significantly elevated in KICH, PCPG, READ, and LGG. Conversely, CESC and SARC demonstrated a notable increase in the frequency of heterozygous amplification of the DNAJB4 gene.

(E) Homozygous deletions of DNAJB4 were predominantly identified in PRAD and PCPG, whereas homozygous amplifications were chiefly observed in OV, SARC, UCS, and BRCA.

(F) CNV of DNAJB4 was significantly correlated with OS in BRCA, UCEC, LGG, KIRC, SARC, and KIRP. Furthermore, it was associated with DFI in DLBC, SARC, KIRP, and COAD. Additionally, CNV of DNAJB4 demonstrated a significant correlation with PFS in UVM, AAC, UCEC, LGG, KIRC, SARC, KIRP, and COAD while also being linked to DSS in BRCA, UCEC, LGG, KIRC, SARC, KIRP, and COAD.

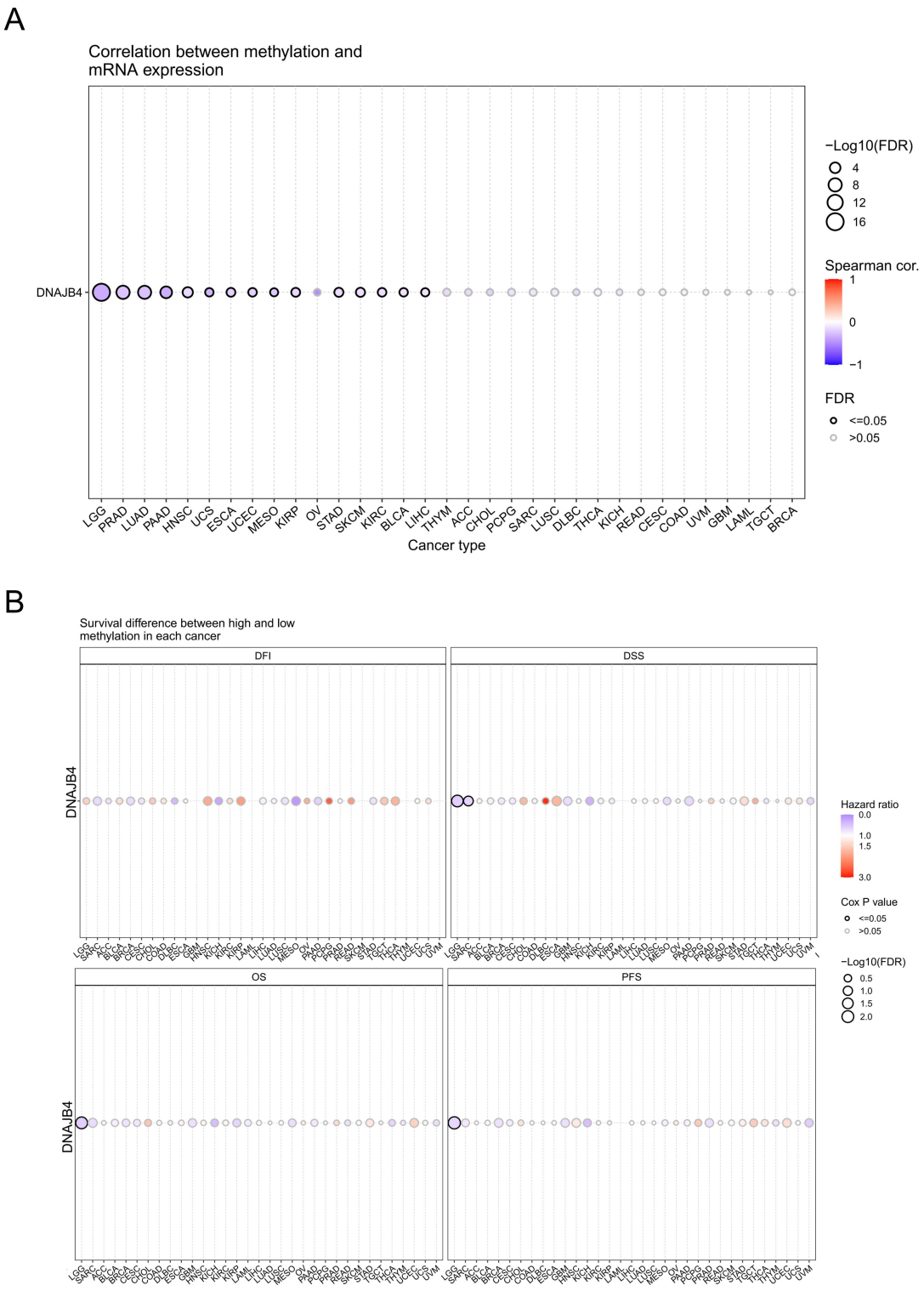

Figure S8. Relationships between DNAJB4 and methylation.

(A) The methylation of DNAJB4 exhibited a negative correlation with the mRNA expression levels in LGG, PRAD, LUAD, PAAD, HNSC, UCS, ESCA, UCEC, MESO, KIRP, STAD, SKCM, KIRC, BLCA, and LIHC.

(B) Increased methylation levels of DNAJB4 were critical risk factors for DSS in LGG and SARC as well as for OS and PFS in LGG.

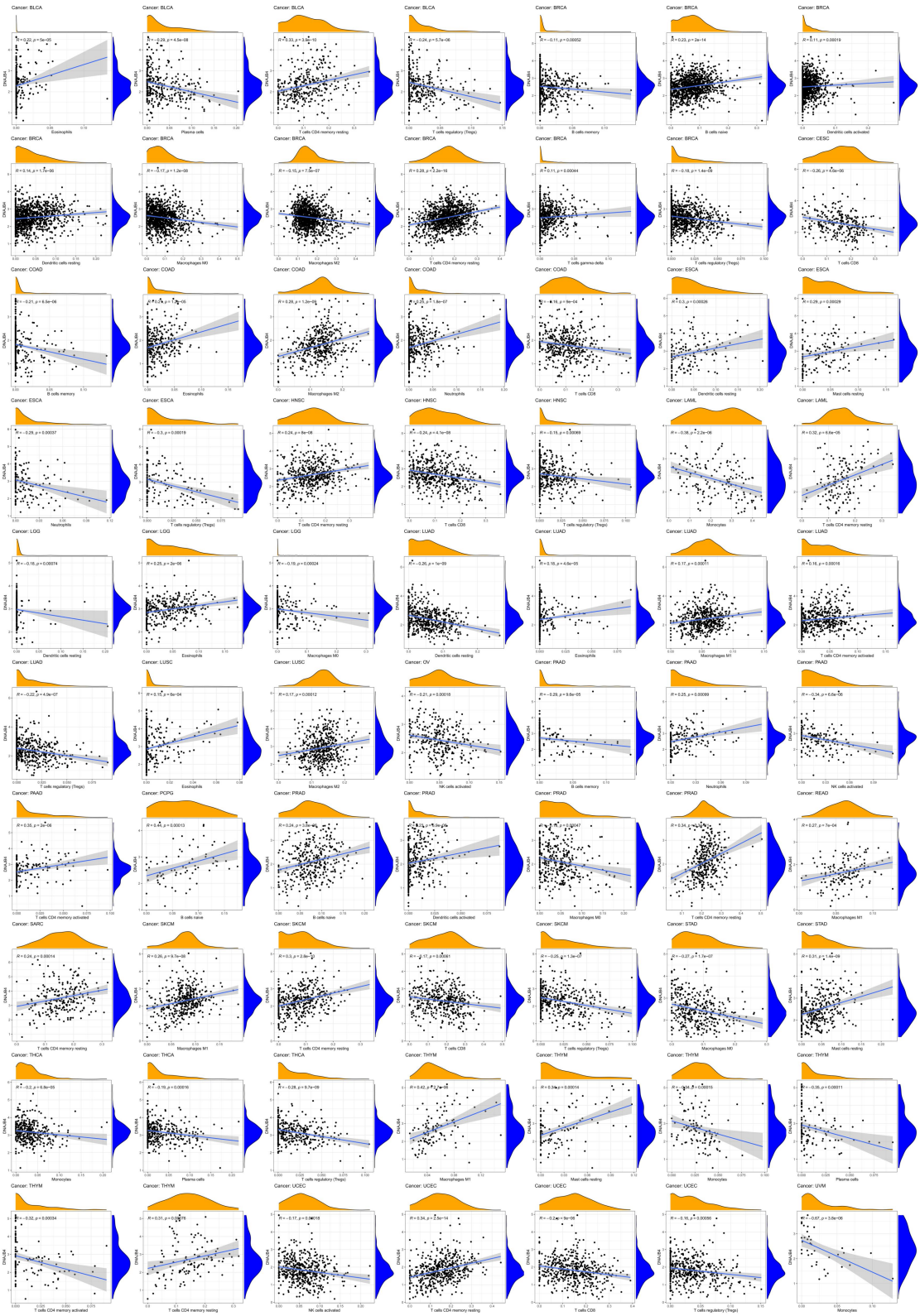

Figure S9. The correlation of DNAJB4 with immune cell infiltration in pan-cancer based on ESTIMATE.

In BLCA, DNAJB4 was positively associated with the infiltration of eosinolhils (R = 0.22, P-value < 0.001) and T cells CD4 memory resting (R = 0.33, P-value < 0.001), but negatively

associated with the infiltration of plasma cells (R = -0.29, P-value < 0.001), and T cells regulatory (R = -0.24, P-value < 0.001). In BRCA, DNAJB4 was positively associated with the infiltration of B cells naive (R = 0.23, P-value < 0.001), dendritic cells activated (R = 0.11, P-value < 0.001), dendritic cells resting (R = 0.14, P-value < 0.001), T cells CD4 memory resting (R = 0.28, P-value < 0.001), and T cells gamma delta (R = 0.11, P-value < 0.001), but negatively associated with the infiltration of B cells memory (R = -0.11, P-value < 0.001), macrophages M0 (R = -0.17, P-value < 0.001), macrophages M2 (R = -0.15, P-value < 0.001), and T cells regulatory (R = -0.18, P-value < 0.001). In CESC, DNAJB4 was negatively associated with the infiltration of T cells CD8 (R = -0.26, P-value < 0.001). In COAD, DNAJB4 was positively associated with the infiltration of eosinophils (R = 0.2, P-value < 0.001), macrophages M2 (R = 0.28, P-value < 0.001), neutrophils (R = 0.25, P-value < 0.001), but negatively associated with the infiltration of B cells memory (R = -0.21, P-value < 0.001), and T cells CD8 (R = -0.16, P-value < 0.001). In ESCA, DNAJB4 was positively associated with the infiltration of dendritic cells resting (R = 0.3, P-value < 0.001), mast cells resting (R = 0.29, P-value < 0.001), but negatively associated with the infiltration of neutrophils (R = -0.29, P-value < 0.001), and T cells regulatory (R = -0.3, P-value < 0.001). In HNSC, DNAJB4 was positively associated with the infiltration of T cells CD4 memory resting (R = 0.24, P-value < 0.001), but negatively associated with the infiltration of T cells CD8 (R = -0.24, P-value < 0.001), and T cells regulatory (R = -0.15, P-value < 0.001). In LAML, DNAJB4 was positively associated with the infiltration of T cells CD4 memory resting (R = 0.32, P-value < 0.001), but negatively associated with the infiltration of monocytes (R = -0.38, P-value < 0.001). In LGG, DNAJB4 was positively associated with the infiltration of eosinophils (R = 0.25, P-value < 0.001), but negatively associated with the infiltration of dendritic cells resting (R = -0.18, P-value < 0.001), and macrophages M0 (R = -0.19, P-value < 0.001). In LUAD, DNAJB4 was positively associated with the infiltration of eosinophils (R = 0.18, P-value < 0.001), macrophages M1 (R = 0.17, P-value < 0.001), T cells CD4 memory activated (R = 0.16, P-value < 0.001), but negatively associated with the infiltration of dendritic cells resting (R = -0.26, P-value < 0.001), and T cells regulatory (R = -0.22, P-value < 0.001). In LUSC, DNAJB4 was positively associated with the infiltration of eosinophils (R = 0.15, P-value < 0.001), and macrophages M2 (R = 0.17, P-value < 0.001). In OV, DNAJB4 was negatively associated with the infiltration of NK cells activated (R = -0.21, P-value < 0.001). In PAAD, DNAJB4 was positively associated with the infiltration of neutrophils (R = 0.25, P-value < 0.001), and T cells CD4 memory activated (R = 0.35, P-value < 0.001), but negatively associated with the infiltration of B cells memory (R = -0.29, P-value < 0.001), and NK cells activated (R = -0.34, P-value < 0.001). In PCPG, DNAJB4 was positively associated with the infiltration of B cells naive (R = 0.44, P-value < 0.001). In PRAD, DNAJB4 was positively associated with the infiltration of B cells naive (R = 0.24, P-value < 0.001), dendritic cells activated (R = 0.23, P-value < 0.001) and T cells CD4 memory resting (R = 0.34, P-value < 0.001), but negatively associated with the infiltration of macrophages M0 (R = -0.18, P-value < 0.001). In READ, DNAJB4 was positively associated with the infiltration of macrophages M1 (R = 0.27, P-value < 0.001). In SARC, DNAJB4 was positively associated with the infiltration of T cells CD4 memory resting (R = 0.24, P-value < 0.001). In SKCM, DNAJB4 was positively associated with the infiltration of macrophages M1 (R = 0.26, P-value < 0.001), and T cells CD4 memory resting (R = 0.3, P-value < 0.001), but negatively associated with the infiltration of T cells CD8 (R = -0.17, P-value < 0.001), and T cells regulatory (R = -0.25, P-value < 0.001). In STAD, DNAJB4 was

positively associated with the infiltration of mast cells resting (R = 0.31, P-value < 0.001), but negatively associated with the infiltration of macrophages M0 (R = -0.27, P-value < 0.001). In THCA, DNAJB4 was negatively associated with the infiltration of monocytes (R = -0.2, P-value < 0.001), plasma cells (R = -0.19, P-value < 0.001), and T cells regulatory (R = -0.28, P-value < 0.001). In THYM, DNAJB4 was positively associated with the infiltration of macrophages M1 (R = 0.42, P-value < 0.001), mast cells resting (R = 0.34, P-value < 0.001) and T cells CD4 memory resting (R = 0.31, P-value < 0.001), but negatively associated with the infiltration of monocytes (R = -0.34, P-value < 0.001), THYM (R = -0.35, P-value < 0.001), T cells CD4 memory activated (R = -0.32, P-value < 0.001). In UCEC, DNAJB4 was positively associated with the infiltration of T cells CD4 memory resting (R = 0.34, P-value < 0.001), but negatively associated with the infiltration of NK cells activated (R = -0.17, P-value < 0.001), T cells CD8 (R = -0.2, P-value < 0.001), and T cells regulatory (R = -0.16, P-value < 0.001). In UVM, DNAJB4 was negatively associated with the infiltration of monocytes (R = -0.67, P-value < 0.001).

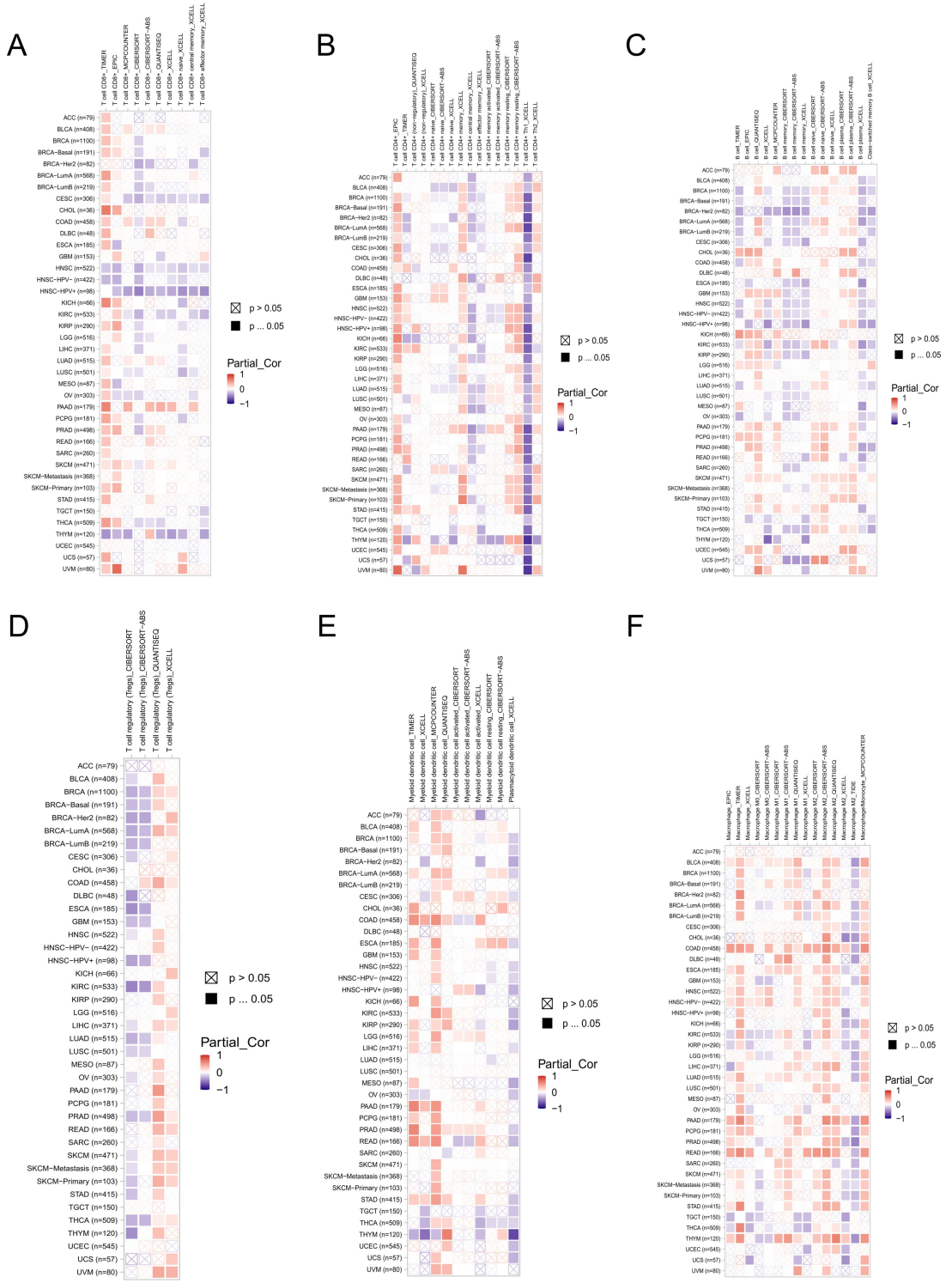

Figure S10. The correlation of DNAJB4 with immune cell infiltration in pan-cancer based on TIMER 2.0.

(A) DNAJB4 was positively associated with the infiltration of T cells CD8+ in BLCA, CHOL, LUAD, PAAD, READ, SARC, SKCM, STAD, UVM, but was negatively correlated in BRCA, CESC, HNSC, KIRC, and THYM.

(B) DNAJB4 was positively associated with the infiltration of T cells CD4+ in ESCA, SKCM, but was negatively correlated in BLCA and THYM.

(C) DNAJB4 was positively associated with the infiltration of B cells in ACC, CHOL, DLBC, KICH, LGG, PAAD, PCPG, SKCM and UVM, but was negatively correlated in BRCA, HNSC, OV.

(D) DNAJB4 was positively associated with the infiltration of T cells regulatory-QUANTISEQ and T cells regulatory-XCELL in pan-cancer but was negatively correlated with T cells regulatory-CIBERSORT and T cells regulatory-CIBERSORT-ABS in pan-cancer.

(E) DNAJB4 was positively associated with the infiltration of myeloid dendritic cell in BLCA, BRCA, COAD, ESCA, PAAD, STAD, but was negatively correlated in THYM.

(F) DNAJB4 was positively associated with the infiltration of macrophage in BLCA, BRCA, COAD, ESCA, HNSC, LUAD, PAAD, PCPG, and READ, but was negatively correlated in KIRC, TGCT, and THCA.

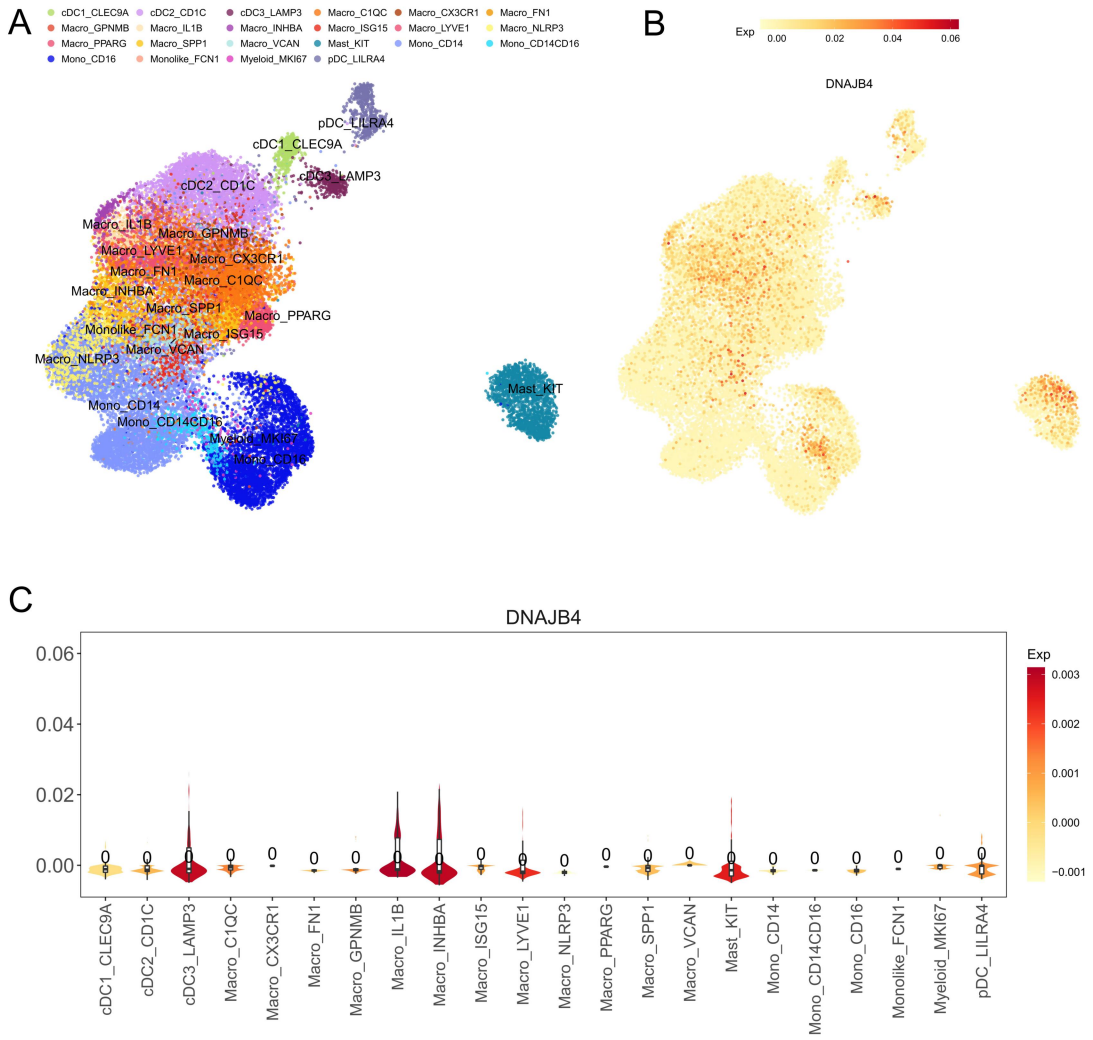

Figure S11. DNAJB4 expression level in myeloid cells

DNAJB4 demonstrated markedly elevated expression levels in specific myeloid cell lines, including cDC3_LAMP3, Macro_IL1B, Macro_INHBA, Macro_LYVE1, and Mast_KIT.

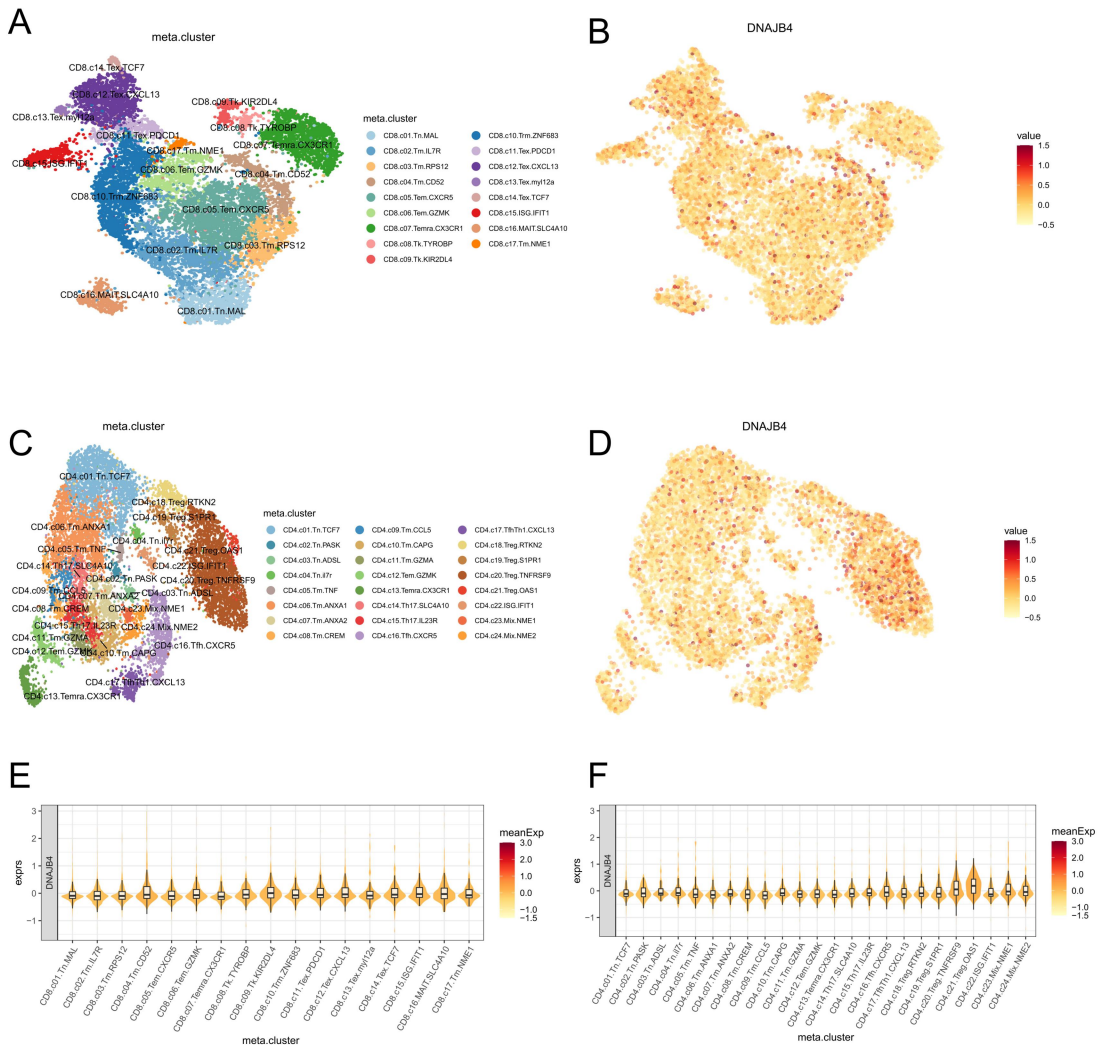

Figure S12. DNAJB4 expression level in T cells

The expression level of DNAJB4 was not significantly different among specific T cell subsets.

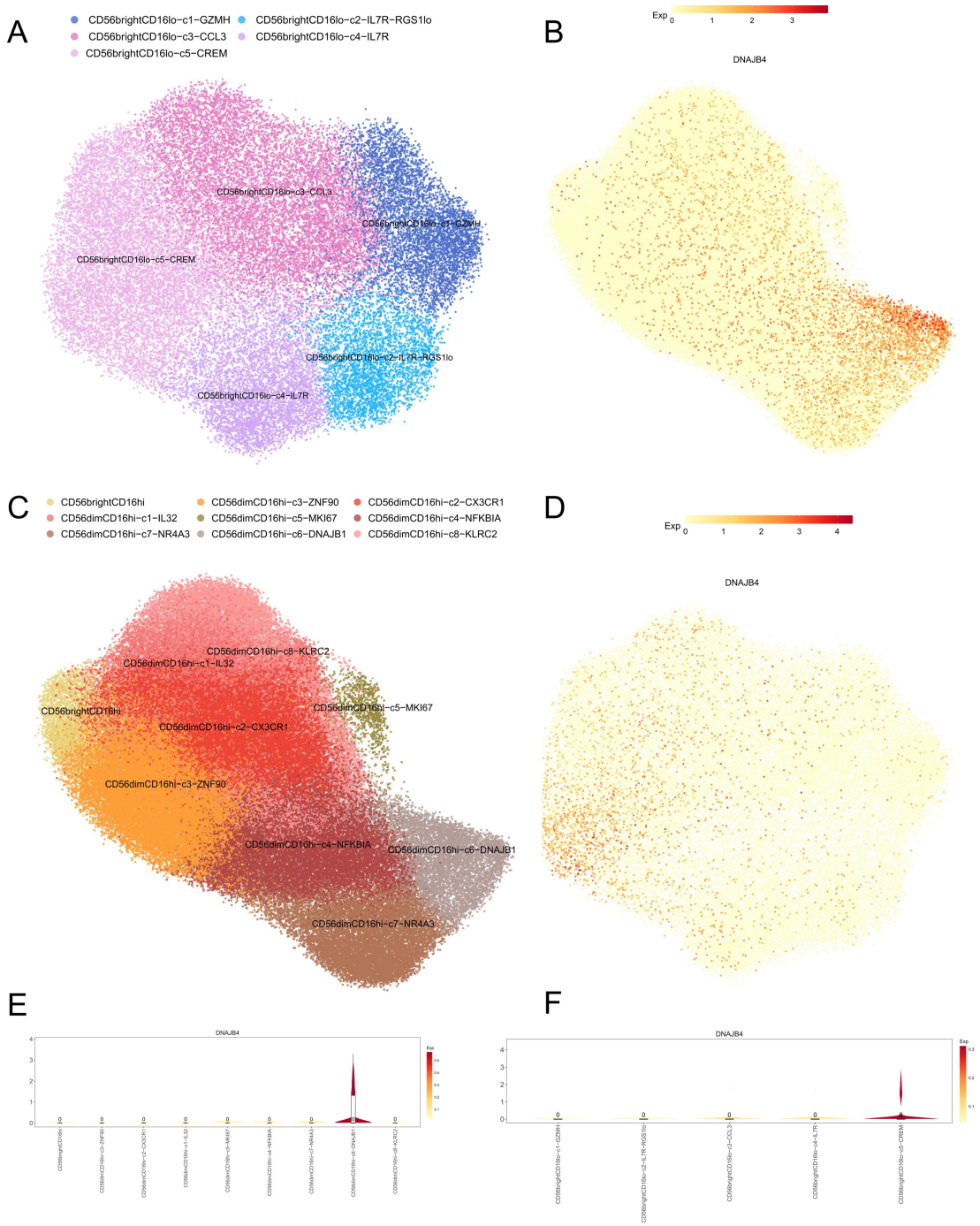

Figure S13. DNAJB4 expression level in NK cells

The expression of DNAJB4 is significantly elevated in CD56dimCD16hi-c6-DNAJB1 and CD56brightCD16lo-c5-CREM.

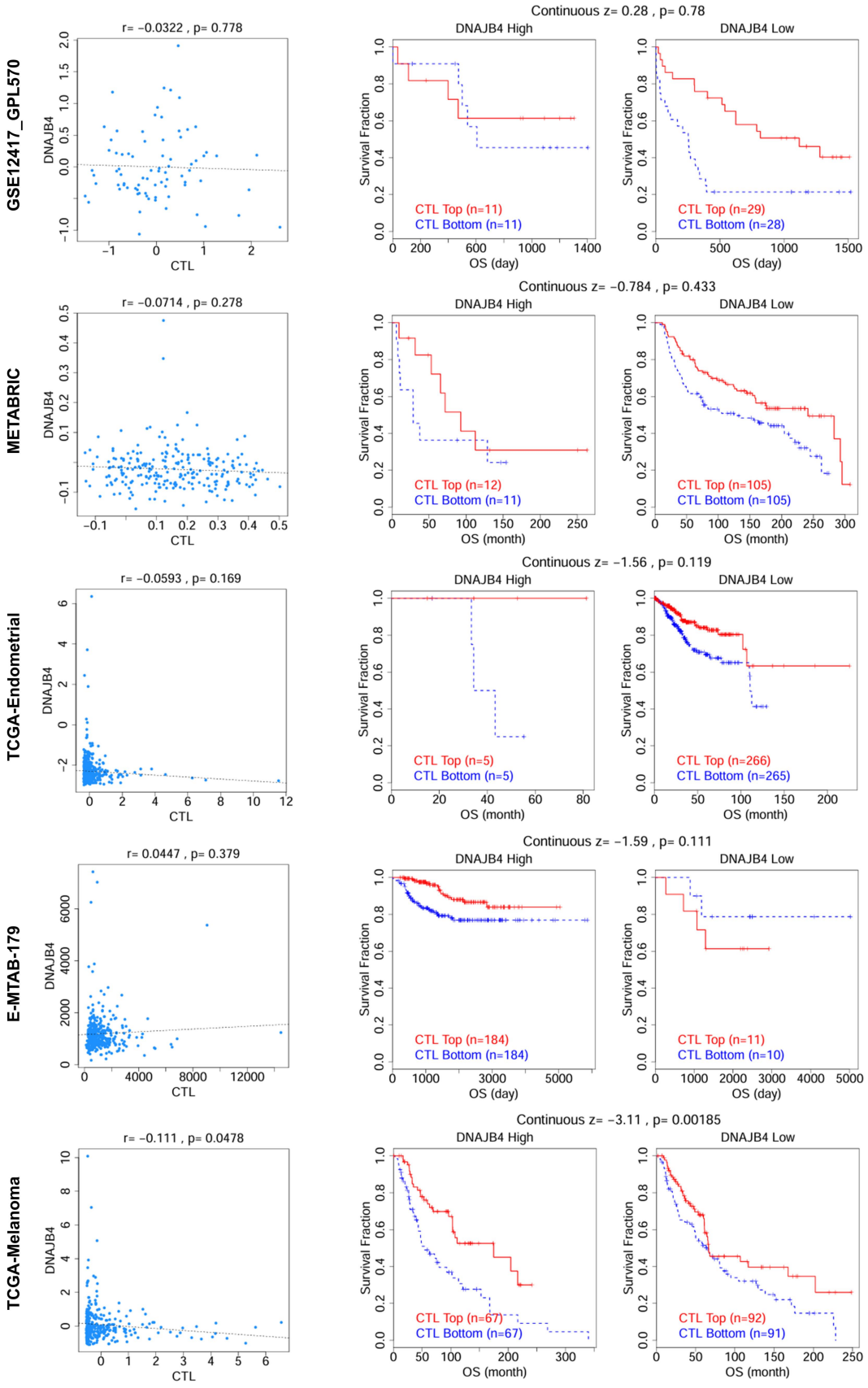

Figure S14. TIDE analysis of DNAJB4 in pan-cancer.

DNAJB4 was negatively correlated with CTL infiltration (R = -0.111, P-value = 0.0478) and T cell dysfunction (Z = -3.11, P-value = 0.00185) in TCGA-Melanoma dataset.

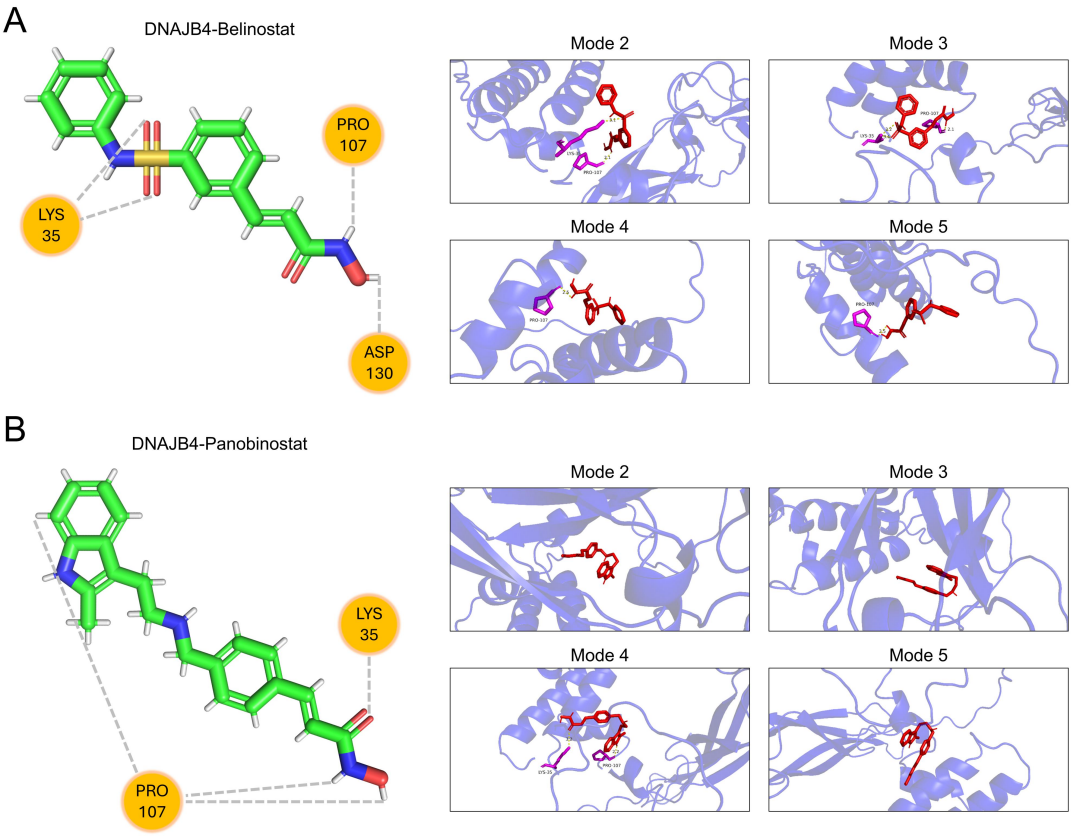

Figure S15. Molecular docking of DNAJB4 with Belinostat or Panobinostat (Mode 2-5).

(A) The Mode 2 (Affinity = -6.5 kcal/mol), Mode 3 (Affinity = -6.5 kcal/mol), Mode 4 (Affinity = -6.5 kcal/mol), Mode 5 (Affinity = -6.5 kcal/mol) of molecular docking between DNAJB4 and Belinostat were exhibited.

(B) The Mode 2 (Affinity = -6.6 kcal/mol), Mode 3 (Affinity = -6.6 kcal/mol), Mode 4 (Affinity = -6.5 kcal/mol), Mode 5 (Affinity = -6.5 kcal/mol) of molecular docking between DNAJB4 and Panobinostat were exhibited.

Figure S16. Demographic and clinical characteristics of 370 patients with kidney neoplasm.

Table S1. Abbreviations of 33 types of cancer in TCGA database.

Abbreviation	Cancer full name
ACC	Adrenocortical carcinoma
BLCA	Bladder urothelial carcinoma
BRCA	Breast invasive carcinoma
CESC	Cervical squamous cell carcinoma and endocervical adenocarcinoma
CHOL	Cholangiocarcinoma
COAD	Colon adenocarcinoma
DLBC	Lymphoid neoplasm diffuse large B-cell lymphoma
ESCA	Esophageal carcinoma
GBM	Glioblastoma multiforme
HNSC	Head and Neck squamous cell carcinoma
KICH	Kidney chromophobe
KIRC	Kidney renal clear cell carcinoma
KIRP	Kidney renal papillary cell carcinoma

LAML	Acute myeloid leukemia
LGG	Brain lower grade glioma
LIHC	Liver hepatocellular carcinoma
LUAD	Lung adenocarcinoma
LUSC	Lung squamous cell carcinoma
MESO	Mesothelioma
OV	Ovarian serous cystadenocarcinoma
PAAD	Pancreatic adenocarcinoma
PCPG	Pheochromocytoma and paraganglioma
PRAD	Prostate adenocarcinoma
READ	Rectum adenocarcinoma
SARC	Sarcoma
SKCM	Skin cutaneous melanoma
STAD	Stomach adenocarcinoma
TGCT	Testicular germ cell tumors
THCA	Thyroid carcinoma
THYM	Thymoma
UCEC	Uterine corpus endometrial carcinoma
UCS	Uterine carcinosarcoma
UVM	Uveal melanoma

Table S2. Demographic and clinical characteristics of the renal cancer cohort

Variables	Number (%)	Mean ± SD; Median (range)	P-value
DNAJB4 tumor		6.78 ± 3.11; 8 (0-12)	
DNAJB4 classification tumor			
Low (IHC score of DNAJB4 < 6)	149 (40.71)		
Medium (6 <= IHC score of DNAJB4 < 9)	159 (43.44)		
High (IHC score of DNAJB4 >= 9)	58 (15.85)		
Unknown	4 (1.08)		
DNAJB4 normal		8.32 ± 2.47; 8 (2-12)	
DNAJB4 classification normal			< 0.001***
Low (IHC score of DNAJB4 < 6)	43 (14.14)		
Medium (6 <= IHC score of DNAJB4 < 9)	187 (61.51)		
High (IHC score of DNAJB4 >= 9)	74 (24.34)		
Unknown	66 (17.84)		
OS censor			
Alive	276 (74.59)		
Dead	23 (6.22)		
Unknown	71 (19.19)		
OS		42.24 ± 9.34; 41 (7-62)	
OS classification (months)			< 0.05*
High (OS > 41)	134 (45.42)		

Low (OS <=41)	161 (54.58)		
Unknown	75 (20.27)		
PFS censor			
No	257 (69.46)		
Yes	42 (11.35)		
Unknown	71 (19.19)		
PFS		40.90 ± 11.07; 41 (0-62)	
PFS classification (months)			< 0.01**
High (PFS > 41)	134 (36.22)		
Low (PFS <=41)	161 (43.51)		
Unknown	75 (20.27)		
Age (category)			
21-40	33 (8.92)		
41-60	194 (52.43)		
61-88	143 (38.65)		
Gender			
Female	114 (30.81)		
Male	256 (69.19)		
KIRC			
Yes	328 (88.65)		
No	42 (11.35)		
Histopathological classification			
KIRC	328 (88.65)		
KIRP	18 (4.86)		
KICH	8 (2.16)		
Others	16 (4.32)		
Fuhrman nuclear stage			
Stage 1	69 (18.65)		
Stage 2	234 (63.24)		
Stage 3	51 (13.78)		
Stage 4	16 (4.32)		
T stage			
T1	282 (76.22)		
T2	29 (7.84)		
T3	53 (14.32)		
T4	3 (0.81)		
Unknown	3 (0.81)		
Detailed T stage			
T1a	178 (48.11)		
T1b	104 (28.11)		
T2a	17 (4.59)		
T2b	12 (3.24)		
T3a	49 (13.24)		

T3b	2 (0.54)
T3c	2 (0.54)
T4	3 (0.81)
Unknown	3 (0.81)
N stage	
N0	368 (99.46)
N1	2 (0.54)
M stage	
M0	370 (100.00)
Stage	
Stage 1	282 (76.22)
Stage 2	28 (7.57)
Stage 3	54 (14.59)
Stage 4	3 (0.81)
Unknown	3 (0.81)
Progression after treatment	
Yes	41 (11.08)
No	258 (69.73)
Unknown	71 (19.19)

P-value referred to the Chi-square results between “DNAJB4 classification tumor” and other variables.